




## Fabrication of fiber-reinforced composites via immersed electrohydrodynamic direct writing in polymer gels

**Yunzhi Xu, and Nathaniel Buettner**, Department of Civil and Environmental Engineering, Northwestern University, 2145 Sheridan Rd, Evanston, IL 60208, USA

**Ange-Therese Akono**, Department of Civil and Environmental Engineering, Northwestern University, 2145 Sheridan Rd, Evanston, IL 60208, USA; Department of Mechanical Engineering, Northwestern University, 2145 Sheridan Rd, Evanston, IL 60208, USA

**Ping Guo** , Department of Mechanical Engineering, Northwestern University, 2145 Sheridan Rd, Evanston, IL 60208, USA

Address all correspondence to Ping Guo at [ping.guo@northwestern.edu](mailto:ping.guo@northwestern.edu)

(Received 15 April 2023; accepted 30 June 2023; published online: 24 July 2023)

### Abstract

Fiber-reinforced composites have provided tremendous opportunities in advanced engineering materials, but the fiber generation and spatial distribution are the most challenging aspects. This paper proposes a novel fabrication approach for fiber-reinforced composites with spatially resolved fiber distribution by combining immersion and near-field electrospinning. The new Immersed Electrohydrodynamic Direct-writing (I-EHD) process makes use of an electrostatic force to draw ultrafine fibers and allows the freestanding of electrospun fibers all inside a liquid matrix. This novel approach enables the dynamic control of fiber morphology and 3D spatial distribution inside the composites, which may lead to future scalable 3D printing of multifunctional composites.

### Introduction

Electrospinning is a highly efficient and versatile approach for generating ultrafine fibers. It offers significant potential for the *in situ* production of fiber reinforcements in composite manufacturing.<sup>[1,2]</sup> The electrospinning method makes use of an electrostatic force to draw a polymer solution or melt into an ultrafine fiber with a diameter ranging from micrometer to nanometer scales.<sup>[3]</sup> The ultrafine fibers are typically collected as non-woven mats (a bulk two-dimensional structure). The lack of ability to form nanofibers into porous and three-dimensional structures has limited the full potential of electrospun fibers as a reinforcing phase. Moreover, the chaotic deposition of electrospun fibers due to bending instability<sup>[4]</sup> of electrospinning jet in air leads to very poor control over the spatial distribution and morphology of the nanofibers inside the matrix.

By immersing the spinneret inside a liquid bath for electrospinning, immersion electrospinning could potentially infuse reinforcing fibers directly into the matrix, which facilitates the control and alignment of the fibers. In spite of not targeting the fabrication of fiber-reinforced composites, immersion electrospinning has been demonstrated to achieve a much-reduced jet speed with less chaotic whipping motion.<sup>[5]</sup> Wang et al.<sup>[6]</sup> and Li et al.<sup>[7]</sup> have shed light on the fiber solidification mechanism in immersion electrospinning as a phase separation process as opposed to the solvent evaporation in conventional electrospinning. In these previous attempts, the collected fiber products were still non-woven mats inside a liquid bath. The ability to fully register fibers in a three-dimensional space inside a liquid bath is still lacking.

Recently, advanced 3D-printing techniques are developed to precisely control the deposition of materials for fabricating complex 3D structures. For instance, direct ink writing (DIW) is an extrusion-based 3D-printing technique where a viscoelastic ink is loaded into a syringe and extruded through a deposition nozzle in a layer-by-layer fashion to build up scaffolds and other 3D geometry on a computer-controlled translational stage.<sup>[8]</sup> Further, embedded 3D printing has brought more versatility by registering larger-scale 3D structures within a supporting bath.<sup>[9,10]</sup> Weeks et al.<sup>[11]</sup> and Román-Manso et al.<sup>[12]</sup> focused on fabricating complex 3D lattice structures by immersing the printing nozzle inside a silicone matrix that solely serves as a supporting phase for free-form printing. Wehner et al.<sup>[13]</sup> incorporated the supporting matrix in the end product and precisely controlled the ink registration to create functional soft robots. Although embedded 3D printing is a versatile technique, the scale of the printed structures is typically limited to millimeters due to the size of the nozzle. This size limitation makes it less than ideal as a reinforcement for composite materials, highlighting the need for innovative methods to achieve three-dimensional registration of ultrafine reinforcing fibers.

Electrohydrodynamic direct-writing (EHD) is an electric field-based printing technique that enables the deposition of micro/nanofibers in a controllable manner to create 2D micropatterns and 3D microstructures.<sup>[14]</sup> EHD process has been explored in applications in various fields, such as energy storage,<sup>[15]</sup> flexible electronics,<sup>[16]</sup> liquid transport,<sup>[17]</sup> etc. Near-field electrospinning (NFES) is a precise EHD process for fabricating high-resolution fiber patterns. NFES takes place in the

linear region of the electrospinning jet, which is typically less than 5 mm from the tip of the spinneret.<sup>[18]</sup> While this technique can be used to construct 3D fiber structures in air via a micro-additive manufacturing process,<sup>[19,20]</sup> it is limited by the layered configuration of the resulting fiber scaffolds. However, with the development of immersion electrospinning, it opens the possibility to initiate near-field electrospinning in a liquid bath, where the surrounding liquid can serve as an omnidirectional collector to control the distribution and orientation of fibers in 3D liquid matrix. Nevertheless, there are still two main challenges to overcome: initiating near-field electrospinning inside a liquid, and the selection of appropriate material and process parameters to enable freeform registration of electrospun fibers.

To address the challenge in composite manufacturing of precise control over the spatial distribution of micro- and nanofibers inside the matrix, we propose a new process termed “Immersed Electrohydrodynamic Direct-writing” (I-EHD). The new process applies near-field electrospinning for its fiber registration control in an immersed electrospinning configuration to directly generate and deposit electrospun fibers to the precise location inside a three-dimensional viscous liquid matrix. The liquid matrix with infused electrospun fibers is then cured to yield fiber-reinforced composites with a controlled 3D spatial distribution of fiber reinforcements. Compared to other EHD processes, where solid substrates are usually adopted and 3D fiber structures are achieved through a layer-by-layer stacking method, the proposed I-EHD process allows freestanding support for deposited fibers provided by the surrounding viscous liquid bath. It further enables the controlled registration of isolated fibers and leads to the potential of manipulating 3D fiber distribution directly within a composite matrix. Meanwhile, the dynamic control of the fiber morphology is inherited from the traditional EHD process through adjusting the process parameters of the I-EHD process. Therefore, this novel approach holds significant potential for constructing architected fiber-reinforced composite materials and opens up new possibilities for designing and manufacturing multifunctional composites with advanced fiber reinforcement.

## Materials and methods

### *Immersed electrohydrodynamic direct-writing (I-EHD)*

In this paper, an innovative electrospinning process, termed Immersed ElectroHydrodynamic Direct-writing (I-EHD), is proposed to generate ultrafine fibers inside a viscous liquid matrix for fiber-reinforced composite manufacturing. Our method combines fiber generation, registration, and integration by one single step in the fabrication of electrospun fiber-reinforced composites. Figure 1(a) shows a schematic of the proposed I-EHD process. The polymer solution is fed to the spinneret using a precision syringe pump, and the tip of the spinneret is immersed completely inside a liquid bath, which also functions as a supporting bath for the electrospun fibers. The spinneret is connected to a positive high-voltage supply.

A metal electrode is embedded at the bottom of the liquid bath (inside the container) and connected to the ground. Therefore, an electric field is generated between the spinneret and the ground inside the liquid to draw the polymer solution into an ultrafine jet, which forms the electrospun fibers upon phase exchange between the polymer solvent and the liquid bath.<sup>[6]</sup> The liquid bath is placed on a precision motion stage to enable the programmable fiber trajectory as needed. During the I-EHD process, the spinneret is kept stationary while the stage is moved according to a programmed trajectory to direct the deposition of electrospun fibers. Different from conventional electrospinning and near-field electrospinning where the bending instability is controlled by the distance between the tip of the spinneret and the grounded solid collector, the bending instability of the electrospinning jet in the proposed I-EHD process is regulated by the applied voltage and the viscosity of the liquid matrix. When the viscosity of the matrix is increased, the viscous liquid matrix prevents the bending instability of the jet from propagating and the surrounding liquid near the spinneret acts as the formless collector for the electrospun fibers. Therefore, the I-EHD process can be tailored to either partially or fully control the fiber registration inside a three-dimensional space.

I-EHD enables the design and manufacturing of versatile fiber-reinforced composites. In this study, fiber-reinforced epoxy composites with different internal fiber structures have been fabricated using the I-EHD process to demonstrate the process viability. Figure 1(b) illustrates the manufacturing routes of two types of fiber-reinforced epoxy composites: locally random and globally controlled fiber distribution and fully controlled 3D fiber structure. A ready-to-cure epoxy resin is served as a liquid bath for I-EHD as well as the matrix of the polymer composites. For locally random and globally controlled distribution of fibers, the needle and stage are kept stationary during the I-EHD process, but the electrospinning is conducted at different locations inside the epoxy matrix for various duration to enable the density variation of fibers. For the composites with programmable 3D fiber structure and controlled trajectory of fibers, the precision stage follows programmed motion during the I-EHD process, allowing controlled deposition and direct-writing of fibers within the matrix. After the I-EHD process, the liquid epoxy matrix with electrospun fibers is cured at room temperature for 12 h to yield hardened electrospun fiber-reinforced epoxy composites. The cured composites are then cut into 3-mm slices for visualization and characterization of the internal structure of the fibers.

### *Materials selection*

In order to successfully achieve I-EHD in a liquid bath, three physical conditions need to be simultaneously considered regarding the material properties: (i) the liquid bath must be dielectric with a low permittivity value; (ii) the liquid bath cannot be a solvent of the electrospinning polymer ink, while it should be miscible with the solvent used for the polymer ink;<sup>[6]</sup> (iii) the viscosity of the liquid matrix should be similar

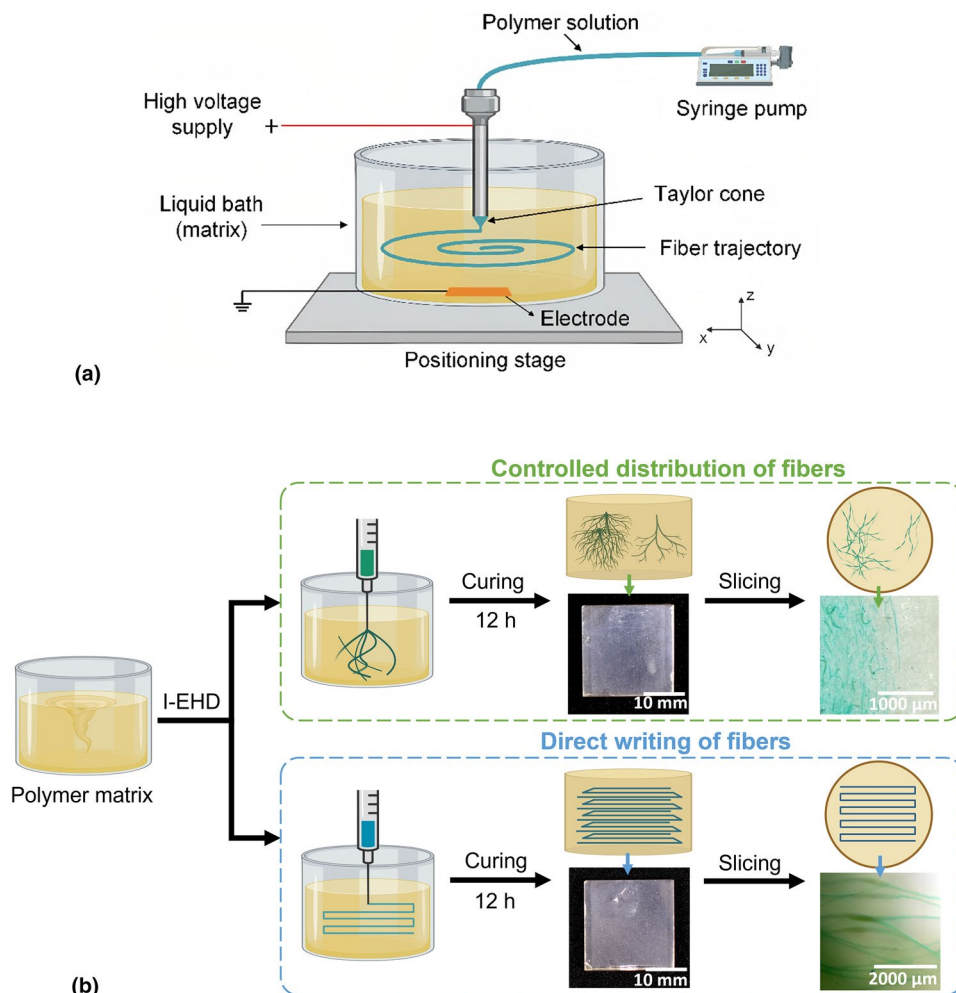


**Figure 1.** Schematics of (a) Immersed Electrohydrodynamic Direct-writing (I-EHD) process; and (b) two manufacturing routes of fiber-reinforced composites enabled by I-EHD process.

to the polymer solution to enable the freestanding of fibers. In this study, a Polyethylene oxide (PEO) solution was used as the I-EHD polymer ink, with the solvent consisting of 70 wt% ethanol. PEO was selected as the polymer for electrospinning due to its low toxicity and ease of handling. In addition, it tends to produce stable electrospun fibers during electrospinning experiments.<sup>[21,22]</sup> The choice to use 70% ethanol as the solvent for PEO was made to increase the miscibility between the polymer solvent and the epoxy matrix, which facilitate the solidification of the electrospun fibers within the liquid matrix. PEO powders with a molecular weight of 600,000 g/mol (Sigma-Aldrich, Burlington, USA) were dissolved in 70% ethanol to prepare the PEO solution with a range of weight ratio from 5 wt% to 15 wt%. The solutions were stirred with a magnetic stirrer for 24 h until homogeneous gels were achieved and pre-dyed for better visualization of the polymer filaments in electrospinning experiments. The liquid bath used in this study was Bisphenol A-based epoxy resin (EpoThin 2, Buehler, Lake Bluff, USA) with a viscosity of approximately

150 Pa·s. The epoxy was mixed with the hardener at a weight ratio of 100 to 45 to form the ready-to-cure resin.

The experimental setup is shown in Fig. 2(a). The PEO solution was loaded in a plastic syringe and extruded using a precision syringe pump (Pump 33 DDS, Harvard Apparatus, Holliston, USA) through a metal needle of gage 25. After the epoxy resin was mixed, the resin was degassed using a vacuum pump to eliminate the air inside the resin and then poured into an acrylic mold with a detachable bottom. A high-voltage DC supply (2K-10, Power Designs Pacific Inc., Palo Alto, USA) with a voltage range of 0 – 2 kV was connected to the needle, and a copper sheet was inserted at the bottom of the container and connected to the ground. The feed rate of the solution was 0.1 mL/h. The distance between the needle tip to the ground was varied between 5 mm and 15 mm based on the applied voltage to maintain a 100 V/mm electric field strength. A digital microscope (Stemi 305, Zeiss, Oberkochen, Germany) was used during the experiments for the observation of I-EHD process.

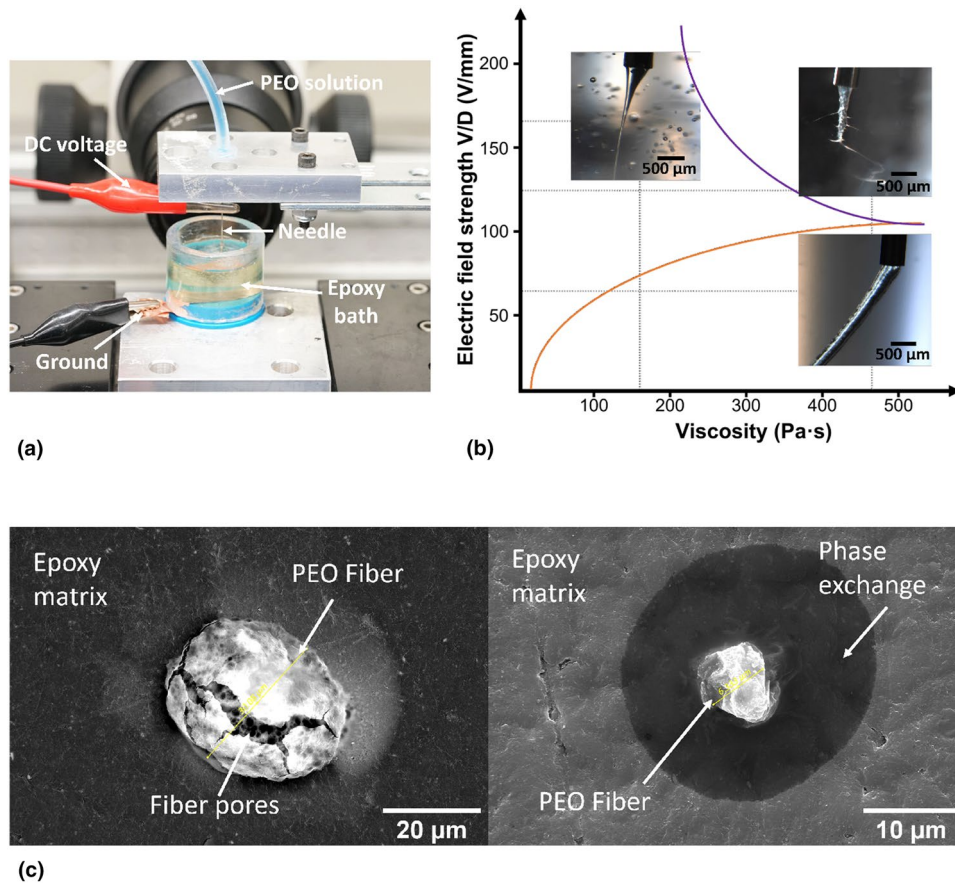


**Figure 2.** (a) Experimental setup of I-EHD process; (b) Process map of I-EHD experiments; (c) SEM images of PEO fibers produced by I-EHD.

### Fiber trajectory programming

In order to achieve a controlled fiber deposition during the I-EHD process, a precision motion stage was controlled by the Labview software with encoded motion programs. A zig-zag fiber trajectory with a longitudinal increment of 20 mm and a transverse increment of 500 μm was prescribed for one single layer of fiber printing. Between each layer, the stage was shifted by 500 μm in the vertical direction to build multi-layer 3D fiber structures inside the coagulation bath.

### Microstructural characterization

To observe the internal microstructure of electrospun fiber-reinforced epoxy composites, the cured samples were cut into 3-mm-thick slices using a diamond saw (Techcut 4, Allied High Tech Products, Compton, CA, USA) and polished down to the level containing electrospun fibers. Optical microscopy and scanning electron microscopy (SEM) were performed to characterize the electrospun fibers generated using I-EHD. Optical microscopy was conducted using a high-resolution optical microscope (AmScope, Irvine, USA) with a magnification of

100X and a stereo microscope (SZ51, Olympus, Tokyo, Japan) with a magnification of 6.5X. For the SEM analysis, the epoxy samples were sputter coated with gold to eliminate the charge on the non-conductive polymer surface. The SEM was performed using an environmental scanning electron microscope (Quanta 650, FEI, Hillsboro, USA) under the high vacuum mode with an applied voltage of 20 kV and a working distance of 10 mm.

### Chemical characterization

The chemical composition of the samples is characterized through Energy-Dispersive X-ray Spectroscopy (EDS) and Fourier-Transform Infrared Spectroscopy (FTIR). EDS was conducted based on the SEM analysis using Quanta 650 environmental scanning electron microscope (FEI, Hillsboro, USA). EDS spectra were collected on the sample surface in the regions of pure epoxy and PEO fibers. FTIR was performed by a Nicolet iS50 FTIR spectrometer (Thermo Fisher Scientific, Waltham, MA, USA) on cured samples. The FTIR spectra were recorded in absorption mode from 4000  $\text{cm}^{-1}$  to 600  $\text{cm}^{-1}$  at a resolution of 4  $\text{cm}^{-1}$  and 64 scans per spectrum.

## Mechanical characterization

Grid nanoindentation testing was performed to characterize the elastic response of the PEO fiber-reinforced epoxy and pure epoxy. Prior to the grid nanoindentation testing, a sample consisting of PEO fibers embedded in epoxy was grinded with a silicon carbide abrasive disk of grit size 180 to expose the PEO fibers. The sample was subsequently grinded with silicon carbon abrasive disks of grit sizes 240, 400, 600, and 1,200. Lastly, the sample was polished with a TexMet polishing cloth using a diamond suspension of  $1\ \mu\text{m}$  size and a soft-woven polishing cloth using a diamond suspension of  $0.25\ \mu\text{m}$  size. For the grid nanoindentation testing, a  $10 \times 40$  grid with a spacing of  $20\ \mu\text{m}$  was employed. Two sets of tests were conducted: (1) in a region with PEO fibers and (2) in a region without PEO fibers. The nanoindentation tests were performed using the Anton-Paar nano-hardness tester equipped with a Berkovich diamond probe to each sample with an increasing vertical force. The maximum vertical force was  $0.75\ \text{mN}$ , loading/unloading rate was  $1.5\ \text{mN/min}$ , and holding phase was  $20\ \text{s}$ . The vertical force and penetration depth measurements were incorporated into the Oliver and Pharr model to calculate the indentation modulus  $M$  and indentation hardness  $H$ .<sup>[23,24]</sup>

$$M = \frac{\sqrt{\pi}}{2} \frac{S}{\sqrt{A(h)}}; H = \frac{P_{\max}}{A(h)}, \quad (1)$$

where  $S$  is the unloading stiffness of the vertical force–penetration depth curve,  $A$  is projected contact area,  $h$  is the penetration depth, and  $P_{\max}$  is the maximum vertical force.

## Results

### Initialization of I-EHD

In order to showcase the process viability of I-EHD, Fig. 2(b) illustrates a process map for the initialization stage of different I-EHD experiments, each with varying concentrations of PEO solutions and process parameters. Two key process parameters are considered in this study—the viscosity of the PEO solution and the electric field strength. The electric field strength was evaluated by  $V/D$ , where  $V$  is the applied voltage and  $D$  is the distance between the needle tip to the bottom of the liquid bath. The PEO solutions used in the experiments were 10 wt% and 15 wt%, with a corresponding zero-shear viscosity of  $188\ \text{Pa}\cdot\text{s}$  and  $475\ \text{Pa}\cdot\text{s}$ , respectively. The results suggested that for 15 wt% PEO solution, when the electric field strength was around  $67\ \text{V/mm}$  ( $V = 1000\ \text{V}$ ,  $D = 15\ \text{mm}$ ), the thinning of the 15 wt% PEO solution jet was limited and a fast extrusion of the polymer solution was observed. With the electric field strength increased to  $120\ \text{V/mm}$  ( $V = 1800\ \text{V}$ ,  $D = 15\ \text{mm}$ ), the electrospinning process was initiated, and multiple bifurcations occurred along the polymer jet. However, the main jet tended to break into segments after the spinning was initiated and no continuous fibers were generated. This can be attributed to the fact that the shear elastic modulus  $G'$  of the 15 wt% PEO solution is too low compared to  $G'$  of the epoxy matrix, which caused

the ink solution to fragment inside the matrix.<sup>[10]</sup> In the case of using 10 wt% PEO solution as the electrospinning solution, the electric field strength applied was  $167\ \text{V/mm}$  ( $V = 500\ \text{V}$ ,  $D = 3\ \text{mm}$ ). A stable and complete electrospinning process was achieved. A Taylor cone<sup>[25]</sup> was formed at the tip of the needle, which signified the initialization of electrospinning. In addition, significant thinning behaviors of the jet were observed, leading to ultrafine electrospun fibers inside the liquid matrix. Therefore, a 10 wt% PEO solution was adopted in the later sections as the electrospinning ink in the I-EHD process.

To investigate the morphology of the PEO fibers produced in I-EHD, the epoxy matrix used in I-EHD was cured for further microstructural characterization. Figure 2(c) displays the SEM images of electrospun PEO fibers found in the cured epoxy matrix. The diameter of the PEO fibers was in the range of  $6 - 30\ \mu\text{m}$ . Small pores with a diameter of  $1 - 2\ \mu\text{m}$  were observed throughout the crack formed on the cross-section of the PEO fiber. This intrinsic porosity of the electrospun PEO fibers resulted from the phase exchange between the polymer solution and the liquid bath (epoxy) during the immersion electrospinning process. This is also confirmed by a second SEM image where an intermediate phase between the fiber and the epoxy matrix is present, which points to the mixing of the solvent and the coagulation bath.

### Controlled distribution of fibers

To demonstrate the versatility of I-EHD process, we first fabricated electrospun PEO fiber-reinforced epoxy composites with globally controlled and locally random distributions of the PEO fibers. This is achieved by changing the electrospinning locations within the epoxy matrix during I-EHD. Figure 3(a) displays the initial and stable stage of the I-EHD process within epoxy where the needle is kept stationary during the experiment. After the voltage was applied, multiple branches of small jets emerged along the main polymer jet, which resulted in a significant reduction of the diameter of the main jet. The stretched main jet then formed a cone-shaped structure with helical fibers due to the bending instability, which was similar to the electrospinning jet behavior in the air.<sup>[26]</sup> However, the speed of the jet was continuously reduced by the viscous epoxy bath, and eventually reached zero, causing the electrospun fibers to be registered in the middle of the liquid bath, without landing on the bottom ground. The optical microscope images of the produced fiber-reinforced composite are shown with different magnification levels. From the microscopic images, the random registration of the electrospun fibers was observed on the cross section of the composite, suggesting a locally random distribution of the electrospun fibers is achieved using I-EHD. Moreover, with a lower magnification, a globally varying distribution of the fibers was displayed, where the blue phases are the fibers and the yellow phase is the epoxy matrix. A clear boundary between the region where I-EHD was taken place and the region where no I-EHD was conducted is observed, which demonstrates that the proposed method is capable of varying and controlling the spatial distribution of fibers inside the matrix material. Image analysis of the microscopic images

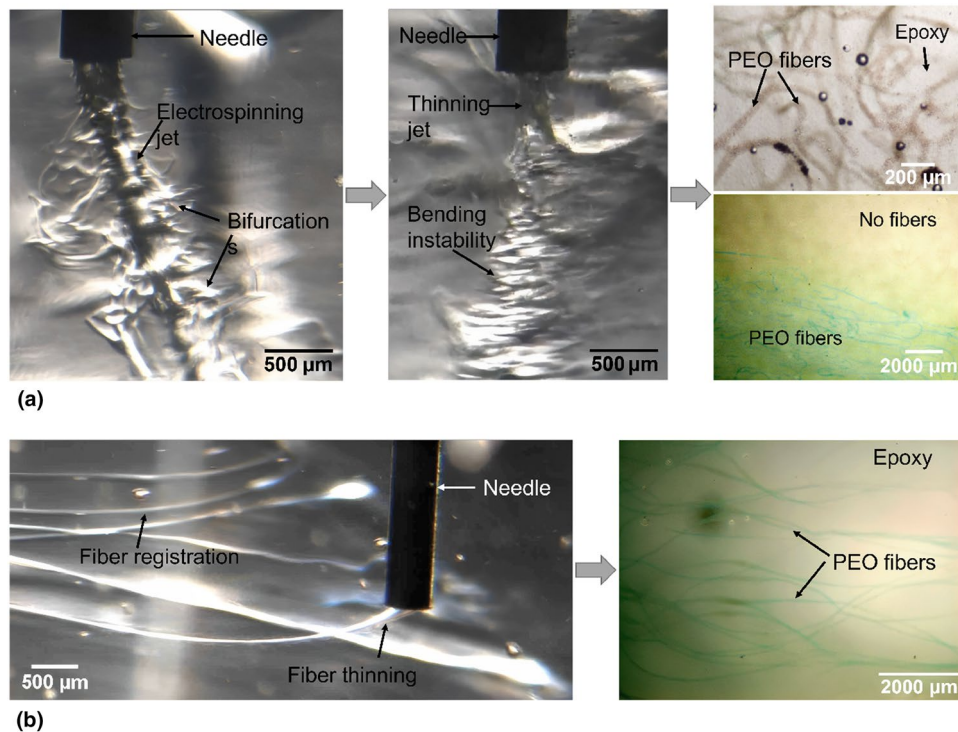


**Figure 3.** I-EHD process and results of (a) controlled distribution of fibers and (b) direct-writing of fibers.

was performed to obtain an average diameter of the electrospun PEO fiber as  $31.62 \pm 7.40 \mu\text{m}$ .

### Direct-writing of fibers

A fully controlled fiber registration was attempted by programming the motion of the stage during the I-EHD process. With the support of the viscous liquid bath, i.e., epoxy resin, the electrospun fibers were able to float inside the liquid matrix instead of settling on the ground. Figure 3(b) shows the stable I-EHD process undergoing the programmed motion inside the matrix. An aligned fiber structure was built with a prescribed zig-zag fiber trajectory. The trajectory featured a longitudinal displacement of 20 mm and a transverse incremental displacement of  $500 \mu\text{m}$ . A single layer of the zig-zag pattern was printed to demonstrate the controllability of the fiber trajectory by the I-EHD method. The produced electrospun fiber pattern is also displayed in Fig. 3(b). An average diameter of the aligned electrospun PEO fibers was calculated as  $19.96 \pm 6.24 \mu\text{m}$ . Aligned electrospun PEO fibers were observed following the zig-zag trajectory. However, after the fibers were printed, the fibers tend to attach to each other due to the residual charges along the polymer solution jet. In future studies, more precise control of the printed fiber structures will be investigated to eliminate any fiber movements after the printing.

### Chemical characteristics

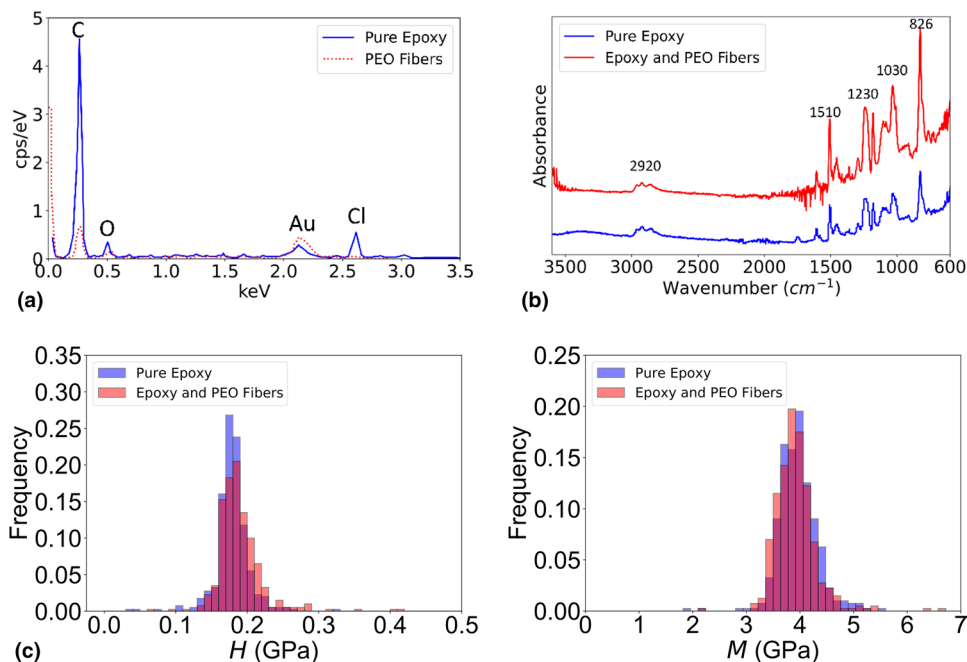
The elemental compositions of the epoxy and PEO fibers are examined through EDS analysis and the results are shown in

Fig. 4(a). The EDS spectrum of pure epoxy shows the presence of carbon, oxygen, and chlorine, for which the weight ratios are 75.8%, 10.1%, and 14.1%, respectively. The presence of gold is due to the sputter coating during the preparation of the specimens for SEM. The EDS spectrum of PEO fibers displays the presence of carbon and oxygen, in the weight ratios of 71.9% and 28.1%, respectively.

Furthermore, the organic groups of the PEO fiber-reinforced epoxy composites are investigated through FTIR analysis, as displayed in Fig. 4(b). The peaks from pure epoxy sustained in epoxy with PEO fibers. The three small peaks in the region of  $2800\text{--}3000 \text{ cm}^{-1}$  are related to C-H stretching vibrations. The peak at  $1610 \text{ cm}^{-1}$ ,  $1510 \text{ cm}^{-1}$ , and  $830 \text{ cm}^{-1}$  are the aromatic bands, which displays a higher intensity in PEO fiber-reinforced epoxy than the pure epoxy. Moreover, the peaks at  $1230 \text{ cm}^{-1}$  and  $1030 \text{ cm}^{-1}$  are assigned to the stretching vibrations of the C-O-C bonds. The intensity of the ether bonds (C-O-C) also increases in the epoxy/PEO composite compared to pure epoxy, which confirms the existence of PEO fibers.<sup>[27]</sup>

### Mechanical properties

The elasto-plastic response of the epoxy samples is evaluated by grid nanoindentation tests. The fabricated PEO fiber-reinforced epoxy composite displays an enhanced indentation hardness compared to pure epoxy. The histograms of indentation hardness  $H$  and indentation modulus  $M$  are shown in



**Figure 4.** (a) EDS spectra, (b) FTIR spectra, (c) mechanical properties of PEO-reinforced epoxy composite.

Fig. 4(c). For pure epoxy, the mean indentation hardness is 179.04 MPa and the mean indentation modulus is 3.96 GPa. With the PEO fibers produced using the I-EHD method, the mean value of indentation hardness and indentation modulus is 189.10 MPa and 3.92 GPa, respectively. A 5.6% increase of hardness is achieved through the reinforcement of PEO fibers, which demonstrates the potential of I-EHD process to produce performance-enhanced fiber-reinforced composites.

## Conclusion

In this study, we proposed an innovative fabrication method, termed Immersed Electrohydrodynamic Direct-writing (I-EHD), to manufacture fiber-reinforced polymer composites with controlled distribution and deposition of ultrafine fibers. Our method uses high electrostatic force to directly generate ultrafine fibers within a viscous liquid matrix and combine fiber generation, registration, and integration within one single step. We demonstrate the process feasibility by directly generating PEO fibers within an epoxy resin matrix. Epoxy composites with a globally controlled and locally random distribution of the electrospun fibers, as well as aligned 3D fiber structure within the matrix were produced. The results suggest that the PEO fiber-reinforced epoxy composite produced by I-EHD displays a similar chemical structure compared to pure epoxy with a higher intensity of the ether linkage. The PEO fibers also lead to a 5.6% increase in the indentation hardness in the final epoxy composite. Our method provides great potential in manufacturing fiber-reinforced composites with

spatially controlled distribution and deposition of ultrafine fibers and will lead to a highly efficient and scalable manufacturing approach for multifunctional fiber-reinforced composites.

## Acknowledgments

This research was partially supported by the National Science Foundation under grant number CNS-2229170 and grant number DMR-1928702. This work was also supported by the National Science Foundation under Grant No. 1747452, which supported Nathaniel Buettner in his Ph.D. studies. This work made use of the EPIC facility of Northwestern University's NUANCE Center, which has received support from the Soft and Hybrid Nanotechnology Experimental (SHyNE) Resource (NSF ECCS-1542205); the MRSEC program (NSF DMR-1720139) at the Materials Research Center; the International Institute for Nanotechnology (IIN); the Keck Foundation; and the State of Illinois, through the IIN.

## Data availability

The authors declare that the data supporting the findings of this study are available within the paper. Additional raw data are available from the corresponding author on reasonable request.

## Declarations

### Conflict of interest

The authors declare no conflict of interest.

## References

1. Y. Xu, P. Guo, A.-T. Akono, Novel wet electrospinning inside a reactive pre-ceramic gel to yield advanced nanofiber-reinforced geopolymer composites. *Polymers* **14**(19), 3943 (2022)
2. M.T. Aljarrah, N.R. Abdelal, Improvement of the mode I interlaminar fracture toughness of carbon fiber composite reinforced with electrospun nylon nanofiber. *Compos. Part B: Eng.* **165**, 379–385 (2019)
3. J. Xue, T. Wu, Y. Dai, Y. Xia, Electrospinning and electrospun nanofibers: methods, materials, and applications. *Chem. Rev.* **119**(8), 5298–5415 (2019)
4. A.L. Yarin, S. Koombhongse, D.H. Reneker, Bending instability in electrospinning of nanofibers. *J. App. Phys.* **89**(5), 3018–3026 (2001)
5. L.M. Shepherd, M.W. Frey, Y.L. Joo, Immersion electrospinning as a new method to direct fiber deposition. *Macromol. Mater. Eng.* **302**(10), 1700148 (2017)
6. X. Wang, K. Nakane, Preparation of polymeric nanofibers via immersion electrospinning. *Eur. Polym. J.* **134**, 109837 (2020)
7. S. Li, B.-K. Lee, Morphological development of immersion-electrospun polymer products based on nonsolvent-induced phase separation. *ACS Appl. Polym. Mater.* **4**(2), 879–888 (2022)
8. M. Saadi et al., Direct ink writing: a 3d printing technology for diverse materials. *Adv. Mater.* **34**(28), 2108855 (2022)
9. J.T. Muth et al., Embedded 3d printing of strain sensors within highly stretchable elastomers. *Adv. Mater.* **26**(36), 6307–6312 (2014)
10. A.K. Grosskopf et al., Viscoplastic matrix materials for embedded 3d printing. *ACS Appl. Mater. Interfaces* **10**(27), 23353–23361 (2018)
11. R.D. Weeks, R.L. Truby, S.G. Uzel, J.A. Lewis, Embedded 3d printing of multimaterial polymer lattices via graph-based print path planning. *Adv. Mater.* **35**(5), 2206958 (2023)
12. B. Román-Manso, R.D. Weeks, R.L. Truby, J.A. Lewis, Embedded 3d printing of architected ceramics via microwave-activated polymerization. *Adv. Mater.* **35**(15), 2209270 (2023)
13. M. Wehner et al., An integrated design and fabrication strategy for entirely soft, autonomous robots. *Nature* **536**(7617), 451–455 (2016)
14. Z. Zhang, H. He, W. Fu, D. Ji, S. Ramakrishna, Electro-hydrodynamic direct-writing technology toward patterned ultra-thin fibers: advances, materials and applications. *Nano Today* **35**, 100942 (2020)
15. J. Zhong et al., Effect of surface treatment on performance and internal stacking mode of electrohydrodynamic printed graphene and its micro-supercapacitor. *ACS Appl. Mater. Interfaces* **15**(2), 3621–3632 (2023)
16. W. Zou et al., Electrohydrodynamic direct-writing fabrication of micro-structure-enhanced microelectrode arrays for customized and curved physiological electronics. *Adv. Mater. Interfaces* **9**(31), 2201197 (2022)
17. S. Wang, X. Mei, S. Wang, B. Xu, Micro/nanofluidic transport by special fibers deposited by electrohydrodynamic direct-writing. *Mater. Des.* **225**, 111518 (2023)
18. X.-X. He et al., Near-field electrospinning: progress and applications. *J. Phys. Chem. C* **121**(16), 8663–8678 (2017)
19. F.-L. He et al., A novel layer-structured scaffold with large pore sizes suitable for 3d cell culture prepared by near-field electrospinning. *Mater. Sci. Eng.: C* **86**, 18–27 (2018)
20. Y.-S. Park et al., Near-field electrospinning for three-dimensional stacked nanoarchitectures with high aspect ratios. *Nano Lett.* **20**(1), 441–448 (2019)
21. W.K. Son, J.H. Youk, T.S. Lee, W.H. Park, The effects of solution properties and polyelectrolyte on electrospinning of ultrafine poly (ethylene oxide) fibers. *Polymer* **45**(9), 2959–2966 (2004)
22. Y. Xu, J. Ndayikengurukiye, A.-T. Akono, P. Guo, Fabrication of fiber-reinforced polymer ceramic composites by wet electrospinning. *Manuf. Lett.* **31**, 91–95 (2022)
23. W. Oliver, Pharr gm. *J. Mater. Res.* **1992**, 7 (1992)
24. W.C. Oliver, G.M. Pharr, An improved technique for determining hardness and elastic modulus using load and displacement sensing indentation experiments. *J. Mater. Res.* **7**(6), 1564–1583 (1992)
25. A.L. Yarin, S. Koombhongse, D.H. Reneker, Taylor cone and jetting from liquid droplets in electrospinning of nanofibers. *J. Appl. Phys.* **90**(9), 4836–4846 (2001)
26. D.H. Reneker, A.L. Yarin, Electrospinning jets and polymer nanofibers. *Polymer* **49**(10), 2387–2425 (2008)
27. A. Doblies, B. Boll, B. Fiedler, Prediction of thermal exposure and mechanical behavior of epoxy resin using artificial neural networks and Fourier transform infrared spectroscopy. *Polymers* **11**(2), 363 (2019)

**Publisher's Note** Springer Nature remains neutral with regard to jurisdictional claims in published maps and institutional affiliations.

Springer Nature or its licensor (e.g. a society or other partner) holds exclusive rights to this article under a publishing agreement with the author(s) or other rightsholder(s); author self-archiving of the accepted manuscript version of this article is solely governed by the terms of such publishing agreement and applicable law.